Available online at www.sciencedirect.com
SCIENCE DIRECT®
Journal of Catalysis 228 (2004) 174–182
JOURNAL OF CATALYSIS
www.elsevier.com/locate/jcat

Heterogeneous catalysed esterification of acetic acid with isoamyl alcohol: kinetic studies

H.T.R. Teo, B. Saha *

Advanced Separation Technologies Group, Department of Chemical Engineering, Loughborough University, Loughborough, Leicestershire, LE 11 3TU, UK

Received 19 July 2004; revised 10 August 2004; accepted 16 August 2004

Available online 29 September 2004

Abstract

Kinetics of heterogeneous catalysed esterification of acetic acid with isoamyl alcohol was studied with a cation-exchange resin catalyst, Purolite CT-175, in a stirred batch reactor to synthesise a value added ester, isoamyl acetate. Physical and chemical characterisation of the catalyst in the form of scanning electron micrographs, Brunauer–Emmett–Teller (BET) surface area measurement, sodium capacity determination, particle size distribution, and pore size distribution was conducted to assess its performance as a catalyst for esterification reaction. The density functional theory (DFT) model was used to analyse the pore size distribution data of the catalyst. Effects of various parameters such as speed of agitation, catalyst particle size, mole ratio of reactants, reaction temperature, catalyst loading, and reusability of the catalyst were studied to optimise the reaction condition. The equilibrium conversion of acetic acid was found to increase slightly with an increase in temperature from 333 to 363 K and also it increased appreciably with an excess of isoamyl alcohol in the reacting system. CT-175 catalyst can be reused without any loss of catalytic performance. The nonideality of each species in the reacting mixture was accounted for by using the activity coefficient via the use of the UNIFAC group contribution method. The kinetic data were correlated with the Langmuir–Hinshelwood–Hougen–Watson model. The surface reaction is the rate-limiting step.

Keywords: Esterification; Ion-exchange resins; Heterogeneous kinetics; Kinetic modeling; Isoamyl acetate; Reactive distillation; Acetic acid recovery

1. Introduction

Aqueous solutions of acetic acid are produced as by-products of many important chemical processes, such as in the manufacture of cellulose esters, terephthalic acid, and dimethyl terephthalate [1]. Moreover, reactions involving acetic anhydride either as a reagent or as a solvent can produce a large amount of acetic acid-containing waste. Among the industrially relevant examples, the process for the manufacture of cellulose acetate from acetylation of cellulose by acetic acid, acetic anhydride, and sulphuric acid is typically associated with a 35% (w/w) aqueous solution of acetic acid as a waste stream. The terephthalic acid process involves the concentration of up to 65% (w/w) acetic acid in water. The process for the synthesis of glyoxal from acetaldehyde and nitric acid has a relatively dilute acetic acid stream (typically 5–20% w/w) as a by-product.

Recovery of acetic acid from these streams is a major problem in both the petrochemical and fine chemical industries. Reactive distillation is a potentially important method of separation for the recovery of acetic acid. Moreover, during the recovery of acetic acid by esterification with isoamyl alcohol, a value added ester (isoamyl acetate) is formed. An additional column will be required for the complete separation of alcohol and ester. The column would not involve water since it has the highest latent heat and hence the energy costs would be minimised.

Conversions for esterification reactions have long been known to be limited by a slow reaction rate and the existence of reversible reactions. In addition to low conversion, the formation of ternary azeotropes between reactants and products in the mixtures of isoamyl alcohol/amyl acetate/water [2]

* Corresponding author. Fax: (+)44-(0)1509-223923.
E-mail address: b.saha@lboro.ac.uk (B. Saha).

0021-9517/$ – see front matter
doi:10.1016/j.jcat.2004.08.018

makes the esterification process difficult to operate economically. The presence of azeotropes also poses difficulty in subsequent purification processes. Reactive distillation is an effective method that has considerable potential for carrying out equilibrium-limited liquid-phase reactions. It is a unit operation that combines chemical reaction and distillation within a single vessel, thereby reducing equipment and recycle costs. Other advantages offered by reactive distillation include high selectivity, reduced energy uses, and reduction or elimination of solvents [3]. The production of methyl acetate is a classic example of successful reactive distillation [4,5]. This method has also been used for the esterification of a fatty acid [6], as well as being devised as a new method to clean industrial water [7]. However, the major disadvantage is that chemical reaction has to show significant conversion at distillation temperature [8].

To accelerate the reaction rate, catalysts are always employed in a liquid-phase esterification. Despite a strong catalytic effect, the use of homogeneous catalyst, e.g., sulphuric acid, suffers from drawbacks [3], such as the existence of side reactions with reactants/products, equipment corrosion, and having to deal with acid-containing waste. Many solid catalysts, e.g., new solid acids and bases [9], ion-exchange resins [10,11], zeolites [12–14], and acidic clay catalysts [15,16], used in heterogeneous reactions have been reported in the literature. Among them, cation-exchange resins are the most commonly used solid acid catalysts in organic reactions [10,11]. The heterogeneous macromolecular network has thus become a crucial and integral part of industrial acid catalysis. Ion-exchange catalysis involves the use of ion-exchange resins (IERs) to promote reactions that are normally catalysed by mineral acids and bases. In many reactions ion exchangers have been found to offer better selectivities towards the desired product(s) compared to homogeneous catalysts. The use of IERs as catalysts holds distinct advantages [17] over catalysis effected by homogeneous catalysts: (a) the purity of the products is higher, as the side reactions can be completely eliminated or are significantly less; (b) the catalyst can be easily removed from the reaction mixture by filtration; (c) the corrosive environment caused by the discharge of acid-containing waste is eliminated. IERs also find good applications in reactive distillation columns (RDCs), wherein they play a dual role of catalyst and a form of tower packing [1]. IERs have been used in esterification [18] as well as the hydrolysis of methyl acetate in a catalytic distillation column [19]. Furthermore, they have also been used for the esterification of acetic acid with methanol [20], liquid-phase esterification of propionic acid with *n*-butanol [21,22], esterification of acetic acid with amyl alcohol [23], esterification of lactic acid with methanol [24], and esterification of acetic acid with butanol [25]. Esterification of formic acid, acrylic acid, and methacrylic acid with cyclohexene in batch and distillation column reactors using ion-exchange resins as catalysts was studied by Saha and Sharma [26]. Very recently, Steinigeweg and Gmehling [27] reported transesterification processes by combination of reactive distillation and pervaporation for the production of *n*-butyl acetate by transesterification of methyl acetate with *n*-butanol. Pervaporation (using Pervap 2255 membranes) was incorporated with reactive distillation for further separation of the methanol–methyl acetate binary mixture that exists in the distillate stream of an RDC. This combination of reactive distillation and pervaporation shifts the equilibrium towards the desired ester product which leads to conversion close to 100% [27].

The ester of isoamyl alcohol, namely, isoamyl acetate, finds wide industrial applications. It is used in large quantities as artificial flavouring (preservative in sodas, soft drinks, etc., banana-flavoured food items, artificially pear-flavoured food articles), as an additive in cigarettes, and as a solvent for tannins, nitrocellulose, lacquers, celluloid, and camphor. It is also used to manufacture celluloid cements, waterproof varnishes, artificial silk, leather, or pearls, photographic films, bronzing liquids and metallic paints, perfuming shoe polish and dyeing, and finishing textiles. In the present study, which is part of a wider project with the aim of designing RDC, the kinetic behaviour of the heterogeneously catalysed esterification of acetic acid with isoamyl alcohol is studied in a stirred batch reactor using Purolite CT-175 (an acidic cation-exchange resin) as a catalyst. The experimental reaction rates obtained in this work were correlated by heterogeneous kinetic models based on single- and dual-site mechanisms. The behaviour of liquid mixtures in the liquid-phase reactions may deviate markedly from that of the ideal solution. The activity coefficients are used in the model to account for the nonideal mixing behaviour of the bulk liquid phase, and the activity coefficients were predicted using the UNIFAC group contribution method [28]. Moreover, the basic investigation of intrinsic reaction kinetics in the presence of an emerging heterogeneous catalyst is very limited for the present system. Hence, we thought that it would be worthwhile to develop a reliable rate expression, which would be applicable over a wide range of operating conditions, and could be conveniently used for the design of an RDC. The emphasis was placed to optimise the reaction condition. The kinetic data were correlated with heterogeneous kinetic models. The present work is directed towards understanding the chemistry of the reaction and obtaining a suitable rate expression and checking its validity under different experimental conditions.

2. Experimental methods

2.1. Materials and catalysts

Acetic acid (99.8%) and isoamyl alcohol (99%) were purchased from Aldrich Chemical Company, Inc. Isoamyl acetate (> 99% purity) was purchased from Fisher Scientific, UK. The purity of the chemicals was verified by gas chromatographic analysis, and they were used without further purification. The cation-exchange resin used in this

Table 1
Summary of physical and chemical properties of CT-175 catalyst

Physical form	Dark spherical beads
Ionic form	H^+
Concentration of acid sites (meq/dry kg min)	4.9
Particle size (μm)	423 < 1% to 1200 < 2%
Porosity (ml/g)	0.4–0.6
Median pore diameter, d_{50}	500–700
Specific surface area (m^2/g)	20–40
Temperature limit (H^+ form)	418 K

study was Purolite CT-175 (a commercial macroreticular sulphonated styrene divinylbenzene resin) supplied courtesy of Purolite International Limited, UK. The wet catalyst was first washed with methanol to remove any water that might be sorbed in the resin catalyst. This step aided in avoiding the collapse of the resin pore structure in the subsequent drying process. The washed catalyst was dried in a vacuum oven at 373 K for 6 h. The dried catalyst was stored in a desiccator until further use. The properties of the catalyst used for the present work are listed in Table 1.

2.2. Catalyst characterisation

Scanning electron micrographs were taken on a Cambridge Instrument stereo scan 360 microscope at room temperature to observe the surface morphology of CT-175 ion-exchange resin catalyst. The normal second electron mode (i.e., not backscattering) was used and the accelerating voltage was set to 10 kV. Prior to analysis, the catalyst sample was dried in a vacuum oven at room temperature, then mounted using PVA glue on an aluminium platform and gold coated.

The size distribution of the CT-175 catalyst was determined using standard-sized sieves (850 μm down to 180 μm). A known amount of CT-175 resin catalyst was accurately weighed and placed in the top sieve. This was then sieved down through the tower of sieves with decreasing sieve diameters. The amount of ion-exchange resin catalyst in each sieve was weighed. This procedure was repeated several times to ensure result reproducibility. The results of the sieve test were then counterchecked using a Malvern Mastersizer. This equipment is used based on the principle of laser diffraction. A representative amount of CT-175 resin was wetted with demineralised water. The sample was agitated with a built-in stirrer and recirculated around a sample loop. The bulk density of CT-175 was measured by filling a volumetric cylinder with a known weight of the catalyst. The measuring cylinder was continuously tapped during filling to ensure that the catalyst was well packed. The true density of the catalyst was measured using a density bottle. The density bottle of known volume was first weighed with water in it. After that, a known weight of CT-175 was added into the density bottle and reweighed. Thus, the volume of water displaced by the catalyst would be known, and the true density of the catalyst could then be determined. Density measurements were made for a 4-g CT-175 resin sample (measurements were made in duplicate and average values are reported).

Surface area and porosity measurements were carried out by the nitrogen adsorption and desorption method using a Micromeritics ASAP 2010 automatic analyser fitted with an optional high-stability 133.3 $N\,m^{-2}$ pressure transducer. A weighed sample of the catalyst was prepared by outgassing for a minimum period of 24 h at 373 K on the degas ports of the analyser. Adsorption isotherms were generated by dosing nitrogen (> 99.99% purity) onto the catalyst contained within a bath of liquid nitrogen at approximately 77 K. Surface area was measured for the linear relative pressure range between 0.05 and 0.15.

2.3. Apparatus and procedure

The kinetic measurement was carried out in a stirred batch reactor. A thermocouple was placed in the reactor to monitor the temperature. The temperature in the reactor was maintained within ±0.5 K. The reactor was charged with a measured amount of acetic acid and isoamyl alcohol. When the reacting mixture reached the desired temperature, the first sample was withdrawn, after which the measured amount of catalyst was added to the mixture in the reactor through the sampling port. This was considered as the starting time of the reaction. The timing of the experimental run was started after the catalyst was added to the reactor. Ion-exchange resin catalyst particles were suspended in the reaction mixture by continuous stirring via the use of a paddle shaft powered by a stirrer motor (IKA-WERKE). Samples of the reaction mixture were withdrawn at regular intervals and analysed in a Pye Unicam 104 gas chromatograph. A separate set of experimental runs under different conditions was performed to validate the model and its parameters. The reactions were performed under reflux conditions. The change in composition with respect to time was noted.

2.4. Analysis

A Pye Unicam 104 gas chromatograph equipped with thermal conductivity detector was used to analyse the composition of the collected samples. The gas chromatograph column was packed with Porapak Q using helium as carrier gas at a flow rate of 6.25×10^{-7} $m^3\,s^{-1}$. The injector and detector block temperatures were maintained at 523 K. The oven temperature was maintained isothermal at 523 K.

3. Mechanism of reaction

Acetic acid reacts with isoamyl alcohol in the presence of CT-175 cation-exchange resin catalyst (a macroreticular sulphonated styrene divinylbenzene resin) to give the ester, isoamyl acetate. It is proposed that the IER catalysed (heterogeneous) esterification also follows the same mechanistic steps of homogeneous acid catalysed reaction [29].

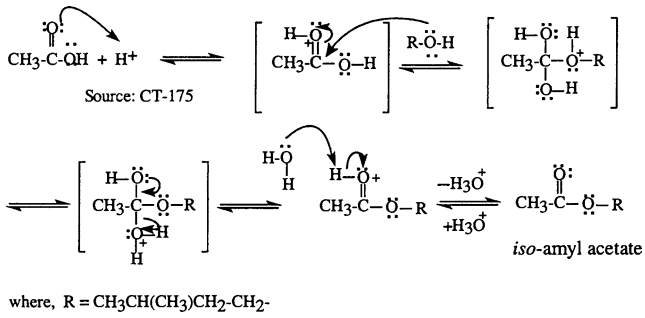

Fig. 1. Mechanism of reaction.

This acid catalysed esterification reaction is an equilibrium-limited chemical reaction:

$$CH_3COOH + (CH_3)_2CHCH_2CH_2OH \Leftrightarrow CH_3COOCH_2CH_2CH(CH_3)_2 + H_2O. \quad (1)$$

In the first step, acetic acid accepts a proton from the strong acid cation exchanger, CT-175. In the second step, the isoamyl alcohol molecule attacks the protonated carbonyl group to give a tetrahedral intermediate. In the next step, a proton is lost at one oxygen atom and gained at another to form another intermediate, which further loses a molecule of water that gives a protonated ester. In the final step, a proton is transferred to a water molecule (acts as a base) to give the ester, isoamyl acetate. All these steps are reversible. The proposed mechanism is shown in Fig. 1. It can be seen from the following section that for the present study, a near-stationary state is reached, tending to equilibrium.

4. Results and discussion

4.1. Catalyst characterisation

Fig. 2 is a scanning electron micrograph of Purolite CT-175 catalyst. Microscopic examination of the morphology of the beads shows agglomerates of microspheres which look like cauliflowers, and each microsphere shows smaller nuclei (10–30 nm) more or less fused together. In between the microspheres, a second family of intermediate pores, i.e., mesopores, is observed (20–50 nm), which may account for moderate surface areas. A third family of large pores (50–1000 nm) is located between the agglomerates. This family, i.e., macropores is responsible for the pore volume of the catalyst. The reactants can permeate easily into these pores irrespective of whether the microspheres are swollen by the reactants.

The particle size distribution of Purolite CT-175 using the sieve test is shown in Fig. 3. It is evident from the results that about 97% (w/w) of the catalyst particles are within the size range 600–850 μm, and the remainder are within the range 180–500 μm. The structure of the polymeric resin bead appears to be robust and the surface of the catalyst appears to be very smooth. The bulk density of CT-175 was calculated to be 0.543 g cm^{-3} and the true density value was 1.95 g cm^{-3}.

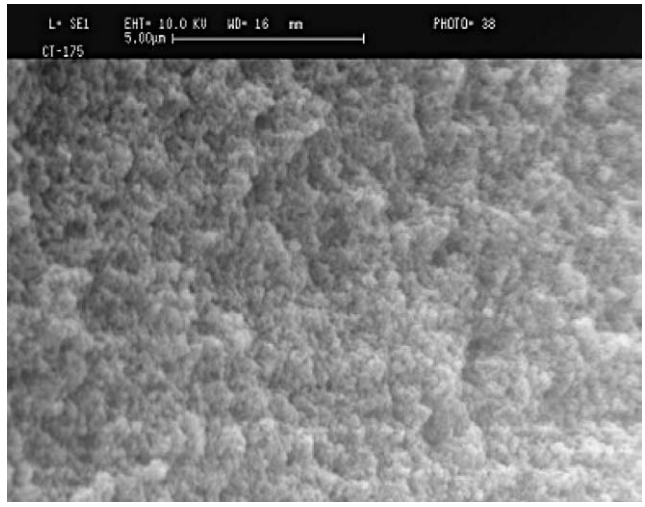

Fig. 2. Scanning electron microscopy image of CT-175 catalyst.

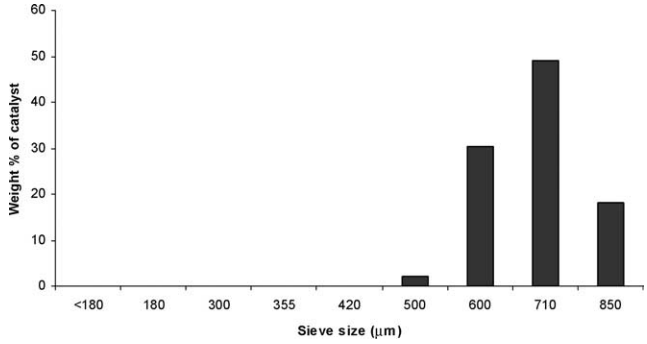

Fig. 3. Particle size distribution of CT-175 catalyst.

Surface area and pore size distribution analysis for all samples was carried out by the N_2 adsorption/desorption method at 77 K. The adsorption isotherm is known to convey a great deal of information about the energetic heterogeneity and geometric topology of the sample under study. The data on physical adsorption have been used for many years as the basis for methods to characterise the surface area and porosity of adsorbents. However, real solid surfaces rarely approach ideal uniformity of structure. It is accepted that, in general, the surface of even nonporous material presents areas of greater or lesser attraction for adsorbed molecules.

This energetic heterogeneity greatly affects the shape of the adsorption isotherm with the result that simple theories such as Langmuir and BET formulas can, at best, give only approximate estimates of surface area. Porous solids virtually are never characterised by a single pore dimension, but instead exhibit a more or less wide distribution of sizes. The observed adsorption isotherm for a typical material is therefore the convolution of an adsorption process with the distribution of one or more properties that affect the process. This was first stated mathematically by Ross and Olivier [30] for the case of surface energy distribution and has become known as the integral equation of adsorption. During the past two decades great advances have been made in the under-

standing of the structure and thermodynamics of inhomogeneous systems of simple molecules, including surface tension and density profile of the free solid surfaces and fluids confined by parallel or cylindrical walls. Density functional theory (DFT) has been especially useful in these investigations, together with computer simulations which can serve a definitive reference [31]. It seems clear that any improved method for extracting micropore and mesopore size information from adsorption data must be as much as possible in accord with these data. As the DFT model is now recognised as a powerful tool for studying inhomogeneous classic fluids [32,33], porosity distribution of the catalyst was calculated using the DFT model based on nitrogen adsorption assuming slit pore geometry. The modelled system consists of a single pore represented by two parallel walls separated by a specific distance. The pore is considered to be open and immersed in a single-component fluid at a fixed temperature and pressure. The fluid responds to the walls and reaches an equilibrium under such conditions. In this condition, by definition, the chemical potential at every point equals the chemical potential of the bulk fluid. The bulk fluid is a homogeneous system of constant density and its chemical potential is determined by the pressure of the system using standard equations. The fluid near the walls is not of constant density and its chemical potential is composed of several position-dependent contributions that must total at every point to the same value as the chemical potential of the bulk fluid. At equilibrium, the entire system has a minimum Helmholtz free energy, thermodynamically known as the grand potential energy. DFT describes the thermodynamic grand potential as a function of the single-particle density distribution, and therefore, calculates the density profile that minimises the grand potential energy and yields the equilibrium density profile.

The calculation method requires the solution of a system of complex integral equations that are implicit functions of the density vector. As analytical solutions are not possible, the problem has been solved using iterative numerical methods. In-depth discussions of DFT and mathematical formulations have been reported by Balbuena and Gubbins [34] and Olivier [32]. Inversion of the integral equation of adsorption to determine micropore size distribution from experimental isotherms using the DFT model usually produces results showing double minima, regardless of the simulation method used. This is assumed to be a model-induced artefact. The inclusion of surface heterogeneity in the model, although more realistic, does not change this observation significantly. The strong packing effects exhibited by a rigid parallel wall model seem likely to be the dominant feature causing the double minima in the derived pore size distributions.

CT-175 is a macroreticular sulphonated styrene divinylbenzene polymeric resin. In the dry state there is very little microporosity in the pore structure. Very prominent access pores (macroporosity) can be seen in the pore size distribution results (see Fig. 4). The measured Brunauer–Emmett–Teller (BET) surface area of CT-175 catalyst sample is 21.3 $m^2\,g^{-1}$ with a pore volume of 0.31 $cm^3\,g^{-1}$.

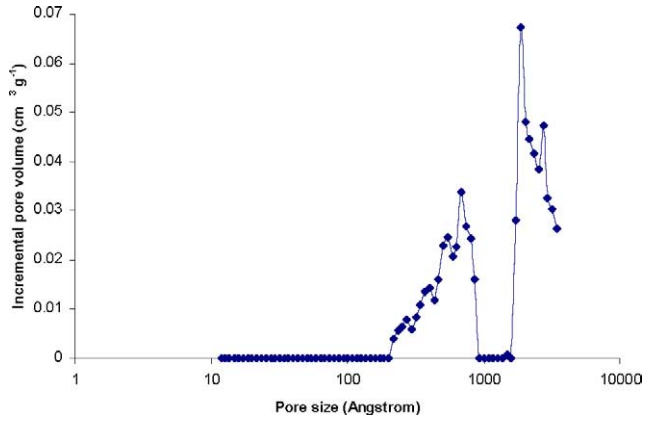

Fig. 4. Pore size distribution of CT-175 catalyst.

4.2. Batch kinetic results

For the ion-exchange resin-catalysed (solid–liquid–liquid mode) reaction, the effect of variables such as the speed of agitation, catalyst particle size, reaction temperature, molar ratio of reactants, catalyst loading, concentration of acetic acid, and reusability of CT-175 catalyst was investigated to optimise the reaction conditions. Detailed information for the batch kinetics study is given below.

4.2.1. Elimination of mass transfer resistances

Preliminary experiments were conducted varying the stirring speed, to quantify the influence of external resistances to heat and mass transfer. These experiments showed that there was very little effect of speed of agitation in the range 300–800 rpm on the overall rate of the reaction. Hence, all further experiments were conducted at a stirrer speed of 500 rpm, ensuring that there were no external mass transfer resistances. It was also confirmed that no attrition of the resin particle took place under the experimental conditions employed for this work.

The effect of particle size was studied using CT-175 catalyst with the particle size range 500–850 μm. For a specified catalyst loading, it was observed that there was no effect of the variation in the particle size from 500 to 850 μm on the rate of reaction. This endorses that intraparticle diffusional resistances of the reactant in the ion-exchange resin are not important. Hence, all further experiments were conducted with the ion-exchange resin that was supplied by the manufacturer (Purolite International Ltd., UK) without any size screening.

4.2.2. Effect of reaction temperature

The study on the effect of temperature is very important for a heterogeneously catalysed reaction as this information is useful in calculating the activation energy for this reaction. Moreover, the intrinsic rate constants are strong functions of temperatures. Fig. 5 presents the variation of conversion

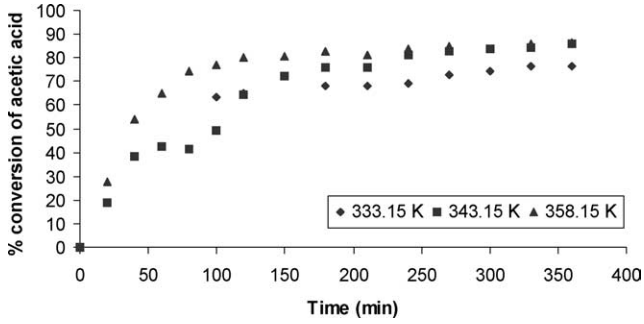

Fig. 5. Effect of temperature on conversion of acetic acid at a catalyst loading of 5% (w/w): feed mole ratio (alcohol to acid), 2:1; catalyst, CT-175; stirrer speed, 500 rpm.

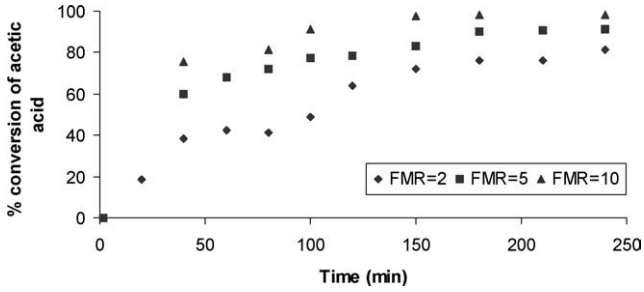

Fig. 6. Effect of feed mole ratio (alcohol to acid) on conversion of acetic acid at a catalyst loading of 5% (w/w): temperature, 343.15 K; catalyst, CT-175; stirrer speed, 500 rpm.

of acetic acid at different reaction temperatures in the range 333.15 to 358.15 K at a feed mole ratio (alcohol to acid) of 1:1, at a stirrer speed of 500 rpm, and at 5% (w/w) CT-175 catalyst loading. It shows that the higher temperature yields the greater conversion of acetic acid at a fixed contact time under otherwise identical conditions. Increasing the temperature is apparently favourable for the acceleration of the forward reaction. However, the equilibrium conversions were nearly equal (about 80% conversion) at the temperatures studied after 6 h.

4.2.3. *Effect of reactant molar ratio*

Esterification of acetic acid with isoamyl alcohol is an equilibrium-limited chemical reaction and because the position of equilibrium controls the amount of ester formed, the use of an excess of isoamyl alcohol increases the conversion of acetic acid. The initial molar ratio of isoamyl alcohol to acetic acid was varied from 2:1 to 5:1 to 10:1 at a temperature of 343.15 K, 5% (w/w) catalyst loading, and stirrer speed 500 rpm. The results are shown in Fig. 6. As observed, the equilibrium conversion increases with the initial isoamyl alcohol-to-acetic acid mole ratio under otherwise identical conditions. The equilibrium conversion of acetic acid increased from about 80% at a feed mole ratio (alcohol to acid) of 2:1 to 95% at a feed mole ratio (alcohol to acid) of 10:1.

4.2.4. *Effect of catalyst loading*

Catalyst loading was varied from 2.5 to 10% (w/w) (i.e., weight of catalyst/total weight of reactants) at a temperature

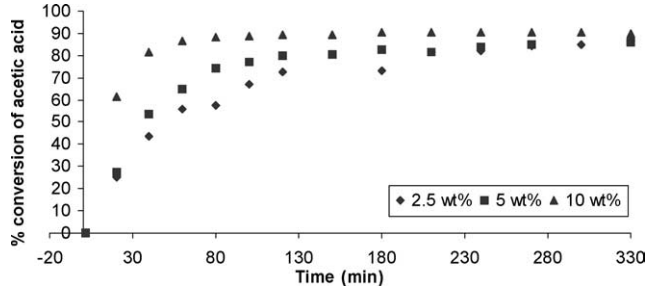

Fig. 7. Effect of catalyst loading on conversion of acetic acid at a feed mole ratio (alcohol to acid) of 2: temperature, 358.15 K; catalyst, CT-175; stirrer speed, 500 rpm.

of 358.15 K, feed mole ratio (θ_{B_0}, alcohol to acid) of 2:1, and stirrer speed of 500 rpm (see Fig. 7). The higher the catalyst loading, the faster the rate at which reaction equilibrium was reached because of the increase in the total number of available active catalytic sites for the reaction. As illustrated in Fig. 7, the rate of acetic acid conversion increased with an increase in catalyst loading from 2.5 to 10% (w/w). For 10% (w/w) catalyst loading, the equilibrium conversion of acetic acid was reached within 1.5 h, whereas for 2.5% catalyst loading it took about 6 h to reach the near-stationary state, tending to equilibrium conversion. It can be seen from Fig. 7 that after about 0.5 h (initial reaction time), the conversion of acetic acid increased from about 30 to 65% with an increase in catalyst loading from 5% (w/w) to 10% (w/w). However, the equilibrium conversion of acetic acid was independent of catalyst loading (after 6 h of reaction). For heterogeneous catalysed reactions, it is not very practical to use more than 10% (w/w) catalyst loading and hence it can be concluded that the optimum catalyst loading based on the current findings was 10% (w/w).

4.2.5. *Effect of catalyst reusability*

IERs are deactivated due to hydrolysis of the functional groups and/or blocking of the active sites as a result of polymerisation or polycondensation products, depolymerisation, and release of oligomeric sulphonic acids because of oxygen sensitivity and desulphonation [35]. Thermal degradation of the resins occurs due to desulphonation and it takes place significantly above 380 K. Fang [36] studied the stability of Amberlyst-15, a macroporous resin, in the temperature range 373–438 K and found that up to 413 K, partial desulphonation occurs and at still higher temperatures, apart from desulphonation, shrinkage of the three-dimensional network takes place, resulting in a hindrance for the access of reactant molecules to active sites. The mechanism and kinetics of desulphonation were studied in detail by Petrus et al. [37]. The desulphonation rate was found to be dependent on the temperature, acid concentration, and charge density on the sulphonic acid group. The kinetic study showed that the process was second order with respect to concentration of sulphonic acid groups. In the present study, macroporous CT-175 resin was reused up to three times (each time for a 6-h run). However, no significant change in the conversion

of acetic acid was observed. Hence, we can infer that CT-175 resin can be used repeatedly for this reaction without sacrificing catalytic activity. According to the manufacturer's specification, the lifetime of ion-exchange resin catalyst is normally about 6000–10,000 operating hours when used at elevated temperatures.

4.2.6. Kinetic modelling

The kinetics of esterification reaction can be expressed using a simple pseudohomogeneous model or more complex models based on the Langmuir–Hinshelwood–Hougen–Watson mechanism (LHHW) or the Eley–Rideal (ER) mechanism [23,25,38,39] in the absence of any intraparticle diffusional limitation. Pseudohomogeneous first- and second-order models are applicable to many ion-exchange resin-catalysed reactions. These models are applicable for highly polar reaction medium. As all the experiments were conducted with ion-exchange resin catalyst, heterogeneous kinetic models, e.g., LHHW and ER models were applied for correlating the kinetic data available at different temperatures, catalyst loadings and mole ratios of acetic acid to isoamyl alcohol.

From a statistical standpoint, the model with the least sum of squares and random residuals would be the most suitable. Moreover, it would be essential that the parameters of the model had a physicochemical meaning and the activation energy was positive.

Reaction rates were calculated by the differential methods as proposed by Cunill et al. [40]. In the case of this heterogeneously catalysed reaction, the equation

$$(-r_A)V = N_{AO}\left(\frac{dX_A}{dt}\right) \tag{2}$$

was used, where $-r_A$ is the reaction rate of acetic acid, V is the reacting mixture volume, N_{AO} is the initial number of moles of acetic acid, X_A is the conversion of acetic acid, and t is the time of the reaction.

To account for the nonideal mixing behaviour of the bulk liquid phase, the activity of the components was taken into account instead of the concentration of the components. The UNIFAC group contribution method was used for estimation of the activity coefficients [41]. Table 2 gives the UNIFAC activity coefficient parameters for all four components at a particular composition.

The equilibrium constant was calculated from the component concentrations at equilibrium through the equation

$$K_{eq} = \left(\frac{a_C a_D}{a_A a_B}\right)_{eq} = \left(\frac{x_C x_D}{x_A x_B}\right)_{eq}\left(\frac{\gamma_C \gamma_D}{\gamma_A \gamma_B}\right)_{eq}, \tag{3}$$

where K_{eq} is the equilibrium constant of the reaction, a is the activity of the component, x is the mole fraction of the component, and γ is the activity coefficient of the component. Subscripts A, B, C, and D denote acetic acid, isoamyl alcohol, isoamyl acetate, and water, respectively.

The parameters for the different models were estimated by minimising the sum of residual squares (SRS) between the experimental and calculated reaction rates using the equation [24]

$$\text{SRS} = \sum_{\text{samples}} (r_{exp} - r_{calc})^2, \tag{4}$$

where SRS is the minimum sum of residual squares resulting in the fitting procedure, and r is the reaction rate. The subscripts exp and calc denote experimental and calculated values, respectively.

Table 2
UNIFAC activity coefficient parameters

Component	Liquid mole fraction, x	Activity coefficient, γ
Acetic acid	0.147	0.872
Isoamyl alcohol	0.476	1.060
Isoamyl acetate	0.189	1.836
Water	0.189	3.259

The LHHW model is applicable whenever the rate-determining step is the surface reaction between adsorbed molecules. On the other hand, the ER model has been applied if in the rate-limiting step, surface reaction takes place between one adsorbed species and one nonadsorbed reactant from the bulk liquid phase. Moreover, because of the strong affinity of resins for water, the activity of water in the catalyst gel phase, where the reaction occurs, is distinctly different from that in the liquid phase [23]. The rate expression for the ER model is

$$-r_A = \frac{A_f\left(\frac{-E_0}{RT}\right)\left(a_A a_B - \frac{A_r}{A_f} a_C a_D\right)}{(1 + K_B a_B + K_D a_D)}, \tag{5}$$

and that for the LHHW model is

$$-r_A = \frac{A_f\left(\frac{-E_0}{RT}\right)\left(a_A a_B - \frac{A_r}{A_f} a_C a_D\right)}{(1 + K_B a_B + K_D a_D)^2}, \tag{6}$$

where A_f and A_r are the Arrhenius preexponential factors for the forward and reverse reactions, respectively, E_0 is the activation energy of the reaction, R is the gas constant, and T is the temperature of the reaction. Parameters K_B and K_D are the adsorption equilibrium constants for amyl alcohol and water, respectively.

It is to be noted that the affinities of CT-175 resin catalyst for water and isoamyl alcohol are stronger than those for acetic acid and isoamyl acetate and hence the adsorption terms for acetic acid and isoamyl acetate are neglected in the LHHW and ER models. Similar models were also proposed by Lee et al. [23] for the study of kinetics of catalytic esterification of acetic acid and amyl alcohol over Dowex 50W catalyst without taking the adsorption terms for both acetic acid and ester into consideration.

The adsorption equilibrium constant for species i, K_i can be defined as the ratio of the adsorption rate constant $k_{a,i}$ to the desorption rate constant, $k_{d,i}$:

$$K_A = \frac{k_{a,A}}{k_{d,A}}, \tag{7}$$

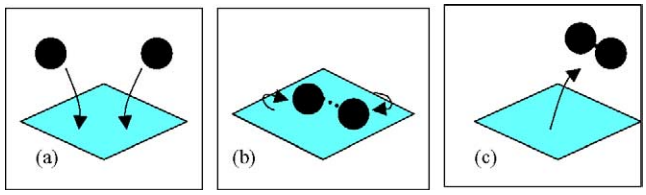

$$A + S \underset{k_{d,A}}{\overset{k_{a,A}}{\rightleftharpoons}} A^*$$
$$B + S \underset{k_{d,B}}{\overset{k_{a,B}}{\rightleftharpoons}} B^*$$
$$A^* + B^* \underset{k_2}{\overset{k_1}{\rightleftharpoons}} C^* + D^*$$
$$C^* \underset{k_{a,C}}{\overset{k_{d,C}}{\rightleftharpoons}} C + S$$
$$D^* \underset{k_{a,D}}{\overset{k_{d,D}}{\rightleftharpoons}} D + S$$

Asterisks indicate the adsorbed species
S represents a vacant active catalyst site

where, A: acetic acid; B: *iso*-amyl alcohol
C: *iso*-amyl acetate; D: water

Fig. 8. Proposed reaction scheme based on LHHW model.

$$K_B = \frac{k_{a,B}}{k_{d,B}}, \tag{8}$$

$$K_C = \frac{k_{a,C}}{k_{d,C}}, \tag{9}$$

$$K_D = \frac{k_{a,D}}{k_{d,D}}. \tag{10}$$

A detailed description for the modelling aspects of heterogeneous acid-catalysed reactions with the LHHW model and the ER model was reported elsewhere [38,42–44]. The proposed reaction scheme based on the LHHW model for the present system is shown in Fig. 8. Fig. 9 shows a representation of the LHHW model that was correlated with the experimental kinetic data by minimising the SRS between the experimental and calculated reaction rates through the simplex algorithm [24]. The experiment was conducted at 343.15 K at a feed mole ratio (alcohol to acid) of 2:1, stirrer speed of 500 rpm, and 5% (w/w) CT-175 catalyst loading. It is to be noted that the LHHW model gave a better correlation between the two models adopted because of the smaller differences between the experimental and model reaction rates. Moreover, for all practical purposes, the LHHW model predicts more accurate results on the reaction kinetics studied under different experimental conditions compared with the ER model. Parameters for the LHHW kinetic model used to fit the experimental data are listed in Table 3. The apparent activation energy for the esterification reaction is about 47 kJ mol^{-1}, which is in good agreement with the literature data [23]. On the basis of the experimental results, we assume that the effect of particle size is negligible or that the value of the average effectiveness factor of CT-175 catalyst in the range studied is about unity. Hence, according to the LHHW mechanism, the isoamyl alcohol molecule first chemisorbs on the active site on the internal surface of the

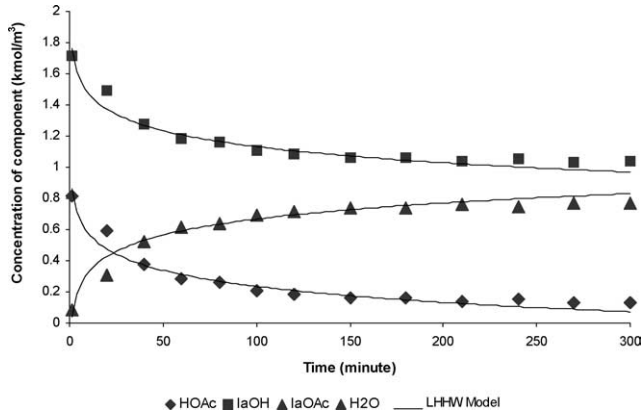

Fig. 9. Comparison between experimental and calculated (with LHHW model) concentration profiles. Feed mole ratio (alcohol to acid), 2:1; temperature, 343.15 K; catalyst, CT-175; catalyst loading, 5% (w/w); stirrer speed, 500 rpm.

Table 3
Parameters for LHHW model used to fit the experimental data

Model	Preexponential factor (mol g^{-1} min^{-1})	Activation energy (kJ/mol)	$K_A a_A$	$K_B a_B$	$K_C a_C$	$K_D a_D$
LHHW	2.4×10^5	47.0	0.23	2.12	0.34	2.21

CT-175 catalyst. It is proposed that the acetic acid molecule also gets adsorbed on the catalyst site and forms an oxonium ion intermediate, which is simultaneously attacked by the isoamyl alcohol adsorbed on the catalyst site (see Fig. 8). During this exchange reaction, isoamyl acetate and water molecules are formed in adsorbed state. All the adsorbed molecules then desorb and give rise to a vacant catalyst site in all cases.

5. Conclusions

The kinetic behaviour for the esterification of acetic acid with isoamyl alcohol in the temperature ranging between 333 and 363 K and at molar feed ratios (of isoamyl alcohol to acetic acid) of 1:1 to 10:1 was investigated experimentally in a stirred batch reactor using Purolite CT-175 catalyst. The optimum condition for synthesising isoamyl acetate has been delineated. The equilibrium conversion of acetic acid was found to increase slightly with an increase in temperature and also it increases appreciably with an excess of isoamyl alcohol in the reacting system. CT-175 catalyst can be repeatedly used without sacrificing its catalytic activity. LHHW and ER kinetic models were applied to correlate with the experimental kinetic data of the solid–liquid–liquid mode catalytic reaction. LHHW model gave a better representation of the kinetic behaviour for all practical purposes on the reaction kinetics studied under the given conditions. According to the LHHW mechanism, acetic acid adsorbed on one catalytic centre reacts with isoamyl alcohol adsorbed on another catalytic centre to give isoamyl acetate and water

each adsorbed on one centre. The surface reaction is the rate-limiting step. The kinetic data for the esterification of acetic acid with isoamyl alcohol would be useful for the simulation and design of a reactive distillation column for removing acetic acid from aqueous streams. We are currently engaged in further studies on esterification of acetic acid with isoamyl alcohol in an RDC bearing in mind the recovery of acetic acid from aqueous streams.

Acknowledgments

This work was funded by EPSRC (GR/N12626). The authors thank Purolite International Limited, UK, especially Dr. Jim Dale, for kindly supplying the catalysts.

Appendix: nomenclature

a	activity
A, B, C, D	acetic acid, isoamyl alcohol, isoamyl acetate, and water, respectively
A_f	Arrhenius preexponential factor for the forward reaction (mol min^{-1} kg^{-1})
A_r	Arrhenius preexponential factor for the reverse reaction (mol $min^{-1}kg^{-1}$)
C_{AO}	initial concentration of acetic acid (mol cm^{-3})
K_A	adsorption equilibrium constant for acetic acid
K_B	adsorption equilibrium constant for isoamyl alcohol
K_C	adsorption equilibrium constant for isoamyl acetate
K_D	adsorption equilibrium constant for water
K_{eq}	equilibrium constant of the reaction
$-r_A$	reaction rate of acetic acid (mol g^{-1} min^{-1})
R	gas constant (kJ mol^{-1} K^{-1})
S	vacant active catalyst site
SRS	minimum sum of residual squares resulting in the fitting procedure
T	temperature (K)
t	time (min)
x_i	mole fraction of component i
X_A	conversion of acetic acid
γ	activity coefficient
θ_{B_0}	molar ratio of feed (isoamyl alcohol to acetic acid)

Subscripts

calc	calculated values
exp	experimental values

References

[1] B. Saha, S.P. Chopade, S.M. Mahajani, Catal. Today 60 (2000) 147.
[2] L. Berg, A. Yeh, Chem. Eng. Commun. 48 (1986) 93.
[3] M.F. Malone, F. Doherty, Ind. Eng. Chem. Res. 39 (2000) 3953.
[4] V.H. Agreda, L.R. Partin, US patent, 4 435 595, 1984.
[5] V.H. Agreda, L.R. Partin, H.H. William, Chem. Eng. Prog. 8602 (1990) 40.
[6] S. Steinigeweg, J. Gmehling, Ind. Eng. Chem. Res. 42 (2003) 3612.
[7] C.L. Bianchi, V. Ragaini, C. Pirola, G. Carvoli, Appl. Catal. B 40 (2003) 93.
[8] T. Popken, L. Gotze, J. Gmehling, Ind. Eng. Chem. Res. 39 (2000) 2601.
[9] K. Tanabe, M. Misono, Y. Ono, H. Hattori, New Solid Acids and Bases, Kodansha/Elsevier Science, Tokyo/Amsterdam, 1989.
[10] A. Charkrabati, M.M. Sharma, React. Polym. 20 (1993) 1.
[11] M.M. Sharma, React. Funct. Polym. 26 (1995) 3.
[12] W.F. Kladnig, Acta Cient. Venez. 26 (1975) 40.
[13] T.L. Marker, G.A. Funck, T. Barger, U. Hammershaimb, US patent, 5 504 258, 1996.
[14] D.E. Hendriksen, J.R. Lattner, M.J.G. Janssen, US patent, 6 002 057, 1999.
[15] S.R. Chitnis, M.M. Sharma, React. Funct. Polym. 32 (1997) 93.
[16] J.T. Kloprogge, J. Porous Mater. 5 (1998) 5.
[17] M.R. AltIokka, A. Citak, Appl. Catal. A 239 (2003) 141.
[18] J. Savkovicstevanovic, M. Misicvukovic, G. Bonciccaricic, B. Trisovic, S. Jezdic, Sep. Sci. Technol. 27 (1992) 613.
[19] Y. Fuchigami, J. Chem. Eng. Jpn. 23 (1990) 354.
[20] Z.P. Xu, K.T. Chuang, Can. J. Chem. Eng. 74 (1996) 493.
[21] W.T. Liu, C.S. Tan, Ind. Eng. Chem. Res. 40 (2001) 3281.
[22] M.J. Lee, J.Y. Chiu, H.M. Lin, Ind. Eng. Chem. Res. 41 (2002) 2882.
[23] M.J. Lee, H.T. Wu, H.M. Lin, Ind. Eng. Chem. Res. 39 (2000) 4094.
[24] M.T. Sanz, R. Murga, S. Beltran, J.L. Cabezas, Ind. Eng. Chem. Res. 41 (2002) 512.
[25] J. Gangadwala, S. Mankar, S.M. Mahajani, A. Kienle, E. Stein, Ind. Eng. Chem. Res. 42 (2003) 2146.
[26] B. Saha, M.M. Sharma, React. Funct. Polym. 28 (1996) 263.
[27] S. Steinigeweg, J. Gmehling, Chem. Eng. Process. 43 (2004) 447.
[28] A. Fredenslund, R.L. Jones, J.M. Prausnitz, AIChE J. 21 (1975) 1086.
[29] T.W.G. Solomons, C.B. Fryhle, Organic Chemistry, seventh ed., Wiley, New York, 2000, p. 829.
[30] S. Ross, J. Olivier, On Physical Adsorption, Interscience, New York, 1964, chap. 1.
[31] J.P.R.B. Walton, N. Quirke, Chem. Phys. Lett. 129 (1986) 382.
[32] J.P. Olivier, Carbon 336 (1998) 1469.
[33] B. Saha, M. Iglesias, I.W. Cumming, M. Streat, Solvent Extract. Ion Exchange 18 (2000) 133.
[34] P.B. Balbuena, K.E. Gubbins, Fluid Phase Equilibria 76 (1992) 21.
[35] W. Neier, Ion exchangers as catalysts, in: K. Dorfner (Ed.), Ion Exchangers, Walter de Gruyter, 1991, p. 981.
[36] F.T. Fang, in: Proceedings of the Third International Congress on Catalysis, Amsterdam, The Netherlands, vol. 2, 1964, p. 90.
[37] L. Petrus, E.J. Stamhuis, G.E.H. Joosten, Ind. Eng. Chem. Prod. Res. Des. 20 (1981) 366.
[38] B. Saha, M.M. Sharma, React. Funct. Polym. 34 (1997) 161.
[39] B. Saha, M. Streat, React. Funct. Polym. 40 (1999) 13.
[40] F. Cunill, M. Ibbora, C. Fite, J. Tejero, J.F. Izquierdo, Ind. Eng. Chem. Res. 39 (2000) 1235.
[41] R.C. Reid, J.M. Prausnitz, B.E. Poling, The Properties of Gases and Liquids, McGraw–Hill, New York, 1987.
[42] J.J. Carberry, Chemical and Catalytic Reaction Engineering, second ed., McGraw–Hill, New York, 1976.
[43] C. Fite, M. Iborra, J. Tejero, J.F. Izquierdo, F. Cunill, Ind. Eng. Chem. Res. 33 (1994) 581.
[44] D. Parra, J. Tejero, F. Cunill, M. Iborra, J.F. Izquierdo, Chem. Eng. Sci. 49 (1994) 4563.